Journal of Colloid and Interface Science 326 (2008) 196–200

Contents lists available at ScienceDirect

Journal of Colloid and Interface Science

www.elsevier.com/locate/jcis

The head-on colliding process of binary liquid droplets at low velocity: High-speed photography experiments and modeling

Feng-Chao Wang, Jiang-Tao Feng, Ya-Pu Zhao *

State Key Laboratory of Nonlinear Mechanics, Institute of Mechanics, Chinese Academy of Sciences, Beijing 100190, People's Republic of China

ARTICLE INFO

Article history:
Received 15 April 2008
Accepted 1 July 2008
Available online 5 July 2008

Keywords:
Droplet collision
Rebound
Coalescence
Conglutination
Contact time
Hertz contact theory

ABSTRACT

The experimental and theoretical studies are reported in this paper for the head-on collisions of a liquid droplet with another of the same fluid resting on a solid substrate. The droplet on the hydrophobic polydimethylsiloxane (PDMS) substrate remains in a shape of an approximately spherical segment and is isometric to an incoming droplet. The colliding process of the binary droplets was recorded with high-speed photography. Head-on collisions saw four different types of response in our experiments: complete rebound, coalescence, partial rebound with conglutination, and coalescence accompanied by conglutination. For a complete rebound, both droplets exhibited remarkable elasticity and the contact time of the two colliding droplets was found to be in the range of 10–20 ms. With both droplets approximately considered as elastic bodies, Hertz contact theory was introduced to estimate the contact time for the complete rebound case. The estimated result was found to be on the same order of magnitude as the experimental data, which indicates that the present model is reasonable.

1. Introduction

Considerable attention has been focused on droplet collision dynamics over a very wide time span due to its fundamental importance and industrial applications. Pioneering work in droplet collisions dates back to 1879, when Lord Rayleigh noted that small droplets can rebound in collisions with a large pool of water [1,2], and it was pointed out that the failure to achieve coalescence in such circumstances is due to a layer of air trapped between the two colliding surfaces to prevent a true contact. As is well known, droplet collision and coagulation in clouds are helpful for the formation of precipitation of rainfalls. Since the presence of feeble electric forces can enhance the coalescence and formation of larger drops during such collisions, electrical charges in clouds aid in the coalescence of droplets and thus may initiate a rainfall.

Droplet impingement plays an important role in many industrial applications, including ink-jet printing, spray painting and coating, rapid spray cooling of hot surfaces. Recently, raindrops have been used to harvest electric energy for microelectromechanical systems (MEMS) from a piezoelectric system [3]. More recently, the application of droplets has been expanded to the field of biotechnology [4], such as to refill the evaporating droplets and to inject nutrients or biochemical molecules contained in a droplet into another one containing the cells. Comprehensive reviews on the droplet collision dynamics can be found in [5,6]. The collision of a single droplet on a solid surface was studied to understand a fundamental mechanism of the complex problem [7]. Experiments show that when a droplet impacts on a solid surface, it may splash, spread, rebound, partially rebound and so on, due to different wetting properties of the surface and various impact velocities [8]. On a super-hydrophobic surface, the droplet can fully rebound with remarkable elasticity [9–11]. The contact time of a bouncing droplet with different parameters was discussed [12,13].

The collisions of free droplets were investigated as another situation [14]. The Weber number, $We = \rho v^2 R/\gamma$, and the impact parameter, $B = \chi/R$, are the key parameters that determine the behavior of collision of two liquid droplets, where ρ is the liquid density, v is the relative velocity, R is the droplet radius, γ is the surface tension, and χ is the projection of the separation distance between the droplet centers in the direction normal to that of v. Many available experiments suggest that the collision behavior of hydrocarbon drops may differ significantly from that of water drops. Qian and Law [14] obtained a regime map with respect to the Weber number and the impact parameter. Three regimes were observed in the collisions of water droplets: coalescence, off-center separation, and near head-on separation. A single droplet impact on films of the same liquid was also studied. The impact can induce coalescence, splashing, bouncing, and droplet floating on the liquid surface [15–17]. Experiments of droplets colliding onto a liquid layer supported by a solid surface show that bouncing, partial absorption, and total absorption may occur with different Weber numbers [18].

* Corresponding author. Fax: +86 10 6256 1284.
E-mail address: yzhao@imech.ac.cn (Y.-P. Zhao).

0021-9797/$ – see front matter
doi:10.1016/j.jcis.2008.07.002

Polydimethylsiloxane (PDMS) elastomer has been widely used as a versatile material in the fabrication of microfluidic devices, rapid prototyping and nanolithography. The well-known advantages of PDMS include its optical transparency, chemical inertness and non-flammable property [19–21]. Motivated by such practical applications in microfluidics, the head-on collision of a droplet with another one resting on a horizontal PDMS substrate is studied both experimentally and theoretically in the present paper. The colliding process of the two droplets was captured with high-speed photography. Different responses after collision were observed in our experiments. Hertz contact theory was applied in a colliding model and the contact time was estimated for the complete rebound case. The influence of the various impact velocities was also discussed.

2. Materials and methods

2.1. PDMS substrate preparation

Two kinds of solid substrates were adopted in our experiments: PDMS membrane (Sylgard 184, Dow Corning, USA; ratio of the base to curing agent = 10:1) of 1.82 mm in thickness, vacuumed for an hour to remove the trapped air-bubbles; and PDMS films fabricated directly on the indium-tin-oxide (ITO) glass plate of 40 mm × 40 mm × 1.1 mm, cleaned thoroughly by the sonicleaning method. PDMS films were spread onto the ITO glass with spin coating by spin coater (KW-4A). The relationship between the spin speed and thickness of the PDMS film was obtained in our previous research [22]. The thickness of the PDMS film was 7.6 µm, as measured with the Surface Profiler (Dektek II A).

2.2. Experimental details

In our experiment, the droplet was placed on the solid substrate and remained as a drop with a definite contact angle θ between the liquid and solid phases, which was measured with the OCA20 system (precision $\pm 0.1^\circ$) from Dataphysics, Germany, using a sessile drop method. Droplets were dropped to the substrate with a dispense unit containing a syringe needle of the system. When droplet 1 was deposited to the substrate, it kept vibrating for a while before reaching a steady state, and then droplet 2 was dropped and collided with droplet 1 (Fig. 1). The distance between the needle and the solid substrate was denoted by H. In the collision experiments, H varied from 3.8 mm to 18.2 mm, the maximum range obtainable in our experiment. Two kinds of droplets (pure water and soapy water with concentration of 2‰) were tested. The contact angle, which was denoted by θ in Fig. 1, was recorded before each collision. For the pure water droplet, the contact angle is $101.7 \pm 2.1^\circ$; for the soapy water droplet, $67.3 \pm 1.4^\circ$. The entire colliding process was recorded with high-speed photography of 400 FPS (frame per second), under the temperature of 23.0 °C and the relative humidity of 31.0%.

3. Results

Four different types of response after collisions were observed:

(i) Complete rebound: Droplet 2 rebounded completely like an elastic ball.
(ii) Coalescence: The two droplets coalesced directly without rebound, permanently merging into one drop.
(iii) Partial rebound with conglutination: Conglutination occurred when droplet 2 rebounded and the two droplets separated successfully.
(iv) Coalescence accompanied by conglutination: Droplet 2 rebounded and then coalesced with droplet 1 due to the conglutination.

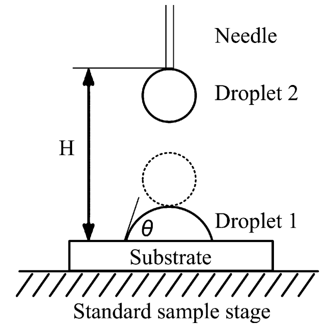

Fig. 1. Schematic diagram of the collision of two droplets.

The governing parameters for the head-on collision of droplets include: the impact velocity v, the droplet radius R, the droplet density ρ, the gravitational acceleration g, the contact angle of droplet 1 with the substrate θ, the surface tension γ and the coefficient of kinetic viscosity μ of the droplets, therefore, for a type of the collision, we will have:

$$f(v, \rho, R, \mu, \gamma, g, \theta) = 0. \tag{1}$$

For the collision of unequal sized drops the ratio of the sizes becomes an important parameter, and for off-center collisions an impact angle must also be considered [23]. In the present paper, we only consider the head-on collision of two isometric droplets of the same fluid.

It is known from Buckingham's Π theorem that there are four independent dimensionless parameters: the Weber number, the Capillary number, the Bond number and the contact angle of droplet 1 with the substrate,

$$f_1(We, Ca, Bo, \theta) = 0. \tag{2}$$

The Weber number, $We = \rho v^2 R/\gamma$, represents the ratio of the inertial force to the surface tension force; the Capillary number, $Ca = \mu v/\gamma$, compares the viscosity force and the surface tension force; the Bond number, $Bo = \rho g R^2/\gamma$, is used to for the effect of gravity of the droplet and is the ratio between the gravity force and the surface tension force. A critical scale of the droplet, namely the capillary length, can be reached when $Bo = 1$. The gravity is neglected in this study because the droplet diameter (taking droplet 2 for instance, the diameter is about 1.3 mm for pure water and 1.1 mm for soapy water) is much smaller than the capillary length (2.7 mm for pure water and 2.0 mm for soapy water). For a certain droplet, the Bond number and the contact angle are essentially fixed; hence the Weber number and the Capillary number are the most important dimensionless parameters, which play a governing role in the response of the collision.

It should be noted that there are some other dimensionless parameters for the wetting behavior, namely, the Ohnesorge number $On = \mu/\sqrt{\rho R \gamma}$, the Reynolds number $Re = \rho v R/\mu$ and the Froude number $Fr = v/\sqrt{gl}$. But, they are not independent. For example, the relation among the Capillary number, the Weber number and the Ohnesorge number can be established as: $On = Ca/\sqrt{We}$; and we also have: $Re = \sqrt{We}/On$ and $Fr = \sqrt{We/Bo}$.

Complete rebounds were observed when a pure water droplet collided with another one resting on the PDMS film coated on ITO glass. The video sequence of this process is displayed in Fig. 2. The impact velocity of droplet 2 was about 0.283 m/s, and $We = 1.47$. In this case, both droplets exhibited remarkable elasticity. A theoretical model will be developed to estimate the contact time in the next section of this paper.

Coalescences (Fig. 3) occurred much more frequently than rebounds. A capillary wave might be generated because of the unbalanced surface tension force. A new droplet might be formed

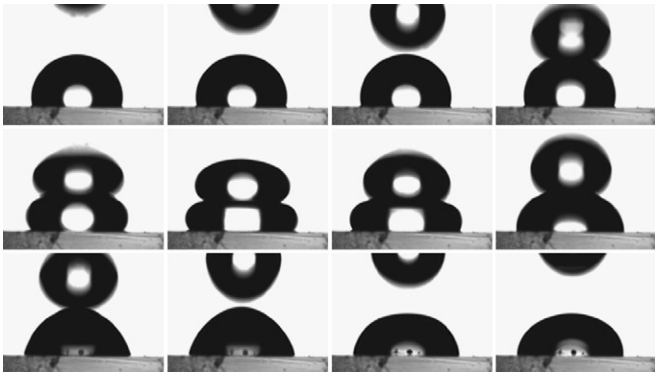

Fig. 2. Snapshots of the collision and rebound of two droplets. $v = 0.283$ m/s, $We = 1.47$. The droplets were of pure water and the solid substrate was PDMS film coated on ITO glass.

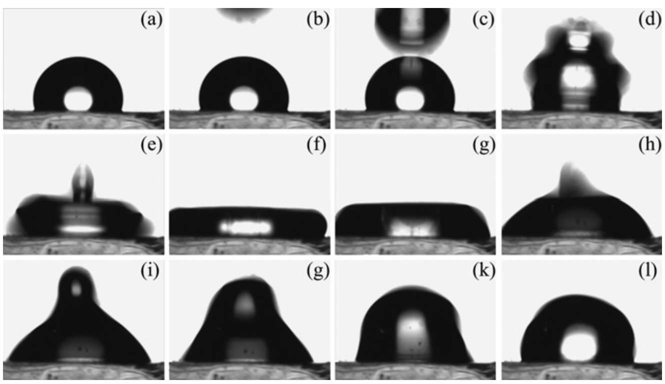

Fig. 3. Snapshots of the collision and coalescences of two pure water droplets. $v = 0.518$ m/s, $We = 4.93$. The solid substrate was the same as that in Fig. 2.

on the top of droplet 2 and its diameter reduced by about a half. The same mechanism might be repeated on the sub-droplet and at least three steps can be seen distinctly in Fig. 3d. The similar phenomenon of "cascade" was also been observed when a droplet impacted on a layer of the same liquid [24] and on a superhydrophobic surface [25].

Conglutinations were also observed during the rebound process sometimes (depicted in Figs. 4 and 5). No visible conglutination was found from Fig. 2 when $Ca = 0.0036$. However, when the soapy water droplets are used, the surface tension γ is reduced remarkably. As a result, both *Ca* and *We* increase. Our experimental results indicated that more conglutinations occurred at larger *Ca* and *We*. Experiments also show that two droplets of soapy water might separate successfully whereas conglutinations occurred (with the corresponding Weber number ranging between 2.99 and 5.12), as shown in Fig. 4. Fig. 5 depicts another case that two pure water droplets coalesced together after the collision by the conglutination. Bremond et al. demonstrated that coalescence occurs during the separation phase and not during the collision [26]. The formation of the "nipples," which was induced by a local low pressure, brought the two interfaces close enough to merge. This region of low pressure is similar with the bubble entrapped during the collision in the surrounding air instead of oil. Air entrapments are frequently captured when a droplet impacts on a liquid surface [27] or on a solid surface [7,28]. These explorations of the behavior of the thin air film may provide the collision response researches with a new angle.

4. Discussion

The head-on collision of two elastic solid spheres at low velocity is a well-known problem according to Hertz elastic contact theory [29]. Based on this approach, Richard et al. measured and estimated the contact time of a bouncing droplet on a hydrophobic surface [12]. As a further study, our experiment observed that the two droplets show remarkable elasticity in the complete rebound case. It inspires us to introduce the Hertz contact theory to describe this colliding and rebound process of two droplets. With details of the collision being obtained with the high-speed photography, a theoretical model can be established to estimate the contact time during which the droplets collide and rebound.

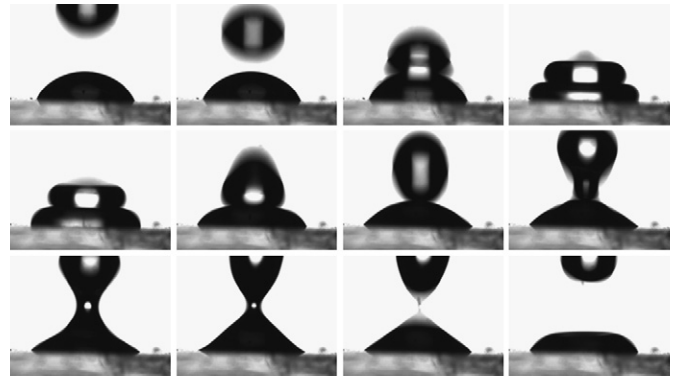

Fig. 4. Snapshots of the collision and rebound of two soapy water droplets. $v = 0.379$ m/s, $We = 4.05$. The solid substrate was PDMS membrane. Conglutinations were observed before two droplets separated successfully.

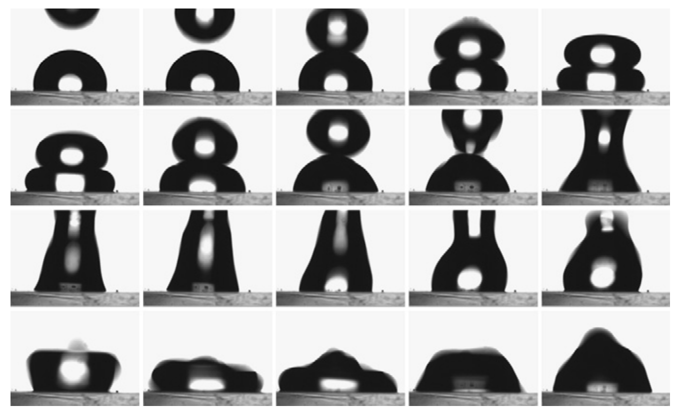

Fig. 5. Snapshots of the collision and coalescence accompanied by conglutination. $v = 0.283$ m/s, $We = 1.47$. The droplets were of pure water and the solid substrate was PDMS film coated on ITO glass.

When two droplets collide together, they approach each other by a short distance h. The surface energy of the two droplets in contact, U, takes the form [30]

$$U = h^{5/2} \frac{2}{5E^*} \sqrt{\frac{R_1 R_2}{R_1 + R_2}}, \qquad (3)$$

where R_1 and R_2 are the curvature radii of the contact surfaces, $E^* = \frac{3}{4}(\frac{1-\sigma_1^2}{E_1} + \frac{1-\sigma_2^2}{E_2})$, E_1, E_2 and σ_1, σ_2 are the Young's moduli and the Poisson's ratios of the two droplets, respectively. The subscripts 1 and 2 indicate quantities pertaining to droplet 1 and droplet 2, respectively.

The Young's modulus and the Poisson's ratio are difficult to define for liquids. We take the Laplace pressure, $E = \gamma / R$ as its equivalent modulus [12]. Substituting $E = \gamma / R$ in the expression of the Weber number, we obtained $We = \rho v^2 / E$, which is the same as the Cauchy number. So the Weber number plays the role of the Cauchy number in this process. The Poisson's ratio of both pure water and soapy water is taken as $\sigma_1 = \sigma_2 = 0.5$ as in an incompressible condition.

We choose a system of coordinates in which the centroid of the two droplets is immobilized. Before collision, the energy of the two droplets is $\xi v^2/2$, where $\xi = m_1 m_2/(m_1+m_2)$ is the reduced mass, v is the relative velocity. The kinetic energy during the collision can be written as $\xi(dh/dt)^2/2$. Based on the energy balance, the loss of kinetic energy converts to the surface energy:

$$\frac{1}{2}\xi v^2 = \frac{1}{2}kh^{5/2} + \frac{1}{2}\xi\left(\frac{dh}{dt}\right)^2, \tag{4}$$

where $k = \frac{4}{5E^*}\sqrt{\frac{R_1 R_2}{R_1+R_2}}$.

The relative velocity of the two droplets is obtained from Eq. (4):

$$\frac{dh}{dt} = \sqrt{v^2 - \frac{kh^{5/2}}{\xi}}. \tag{5}$$

When the relative velocity reduces to zero, the contact droplets reach the maximum approaching distance $h_0 = (\xi/k)^{2/5} v^{4/5}$.

The contact time of the two droplets is twice the time for which h varies from 0 to h_0. Integrating Eq. (5) from $h = 0$ to $h = h_0$, the contact time τ is obtained as

$$\tau = 2\int_0^{h_0} \frac{1}{\sqrt{v^2 - kh^{5/2}/\xi}}\,dh = \frac{4\sqrt{\pi}\,\Gamma(2/5)}{5\Gamma(9/10)}\left(\frac{\xi^2}{k^2 v}\right)^{1/5}, \tag{6}$$

where $\Gamma(*)$ is the Gamma function.

In our model, droplet 1 is rest before collision, so the relative velocity is equal to the impact velocity of droplet 2. The volume of the droplets can be measured experimentally (10.0 μL for pure water and 5.0 μL for soapy water). For these droplets, the radii of curvature of the two contact surfaces R_1 and R_2 will be known from the initial shape. Since the gravity force is neglected for $Bo < 1$, droplet 1 remains in the shape of an approximate spherical segment on the solid substrate and droplet 2 is in the shape of a sphere falling down.

The contact time measured in our experiments for pure water is about 17.5 ms and the theoretical result with our model as calculated by Eq. (6) is about 29.2 ms. The experimental contact time for two soapy water droplets is about 15.0 ms, while the theoretical solution is about 27.0 ms. The analytical solution and the experimental result are on the same order of magnitude, which indicates that the present model is reasonable.

Collisions of soapy water droplets with different impact velocities are shown in Fig. 6. Each frame is taken every 2.5 ms with our present apparatus. According to Eq. (6), the contact time τ varies proportionally to $v^{-1/5}$, as shown in Fig. 7. One can compare the five lines of the phases in Fig. 6 to get the decreasing trend of the contact time with the increase of the impact velocity, which demonstrates the theoretical analysis illustrated in Fig. 7. Richard et al. [12] also introduced another method to estimate the contact time by balancing inertia with capillarity and got $\tau \approx (\rho R^3/\gamma)^{1/2}$. In this sense, the contact time does not depend on the impact velocity over a wide range, which comes up to their experimental result of a liquid droplet impacted onto a super-hydrophobic surface. However, the decreasing trend of the contact time with the increase of the impact velocity ranging between 0.2 m/s and 0.3 m/s can also be found in Fig. 2a of Ref. [12]. The authors think that the phenomena need further discussion.

It should be noted that ours is just a model for an order of magnitude analysis. There are a number of factors neglected, such as: (i) Part of the deformation energy stored in the solid substrate with respect to the overall deformation of the droplets during the collision. (ii) The elastic oscillations of the droplets during the collision. However, to predict the regime precisely and to establish a more detailed model for estimating the contact time motivate us to take ongoing effort working on this study.

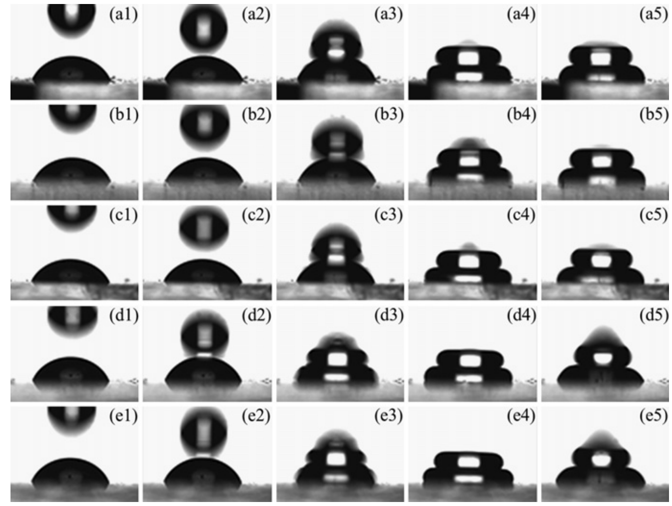

Fig. 6. Soapy water droplets collided together and rebounded with different impact velocities v. (a1)–(a5): $v = 0.326$ m/s, $We = 2.99$. (b1)–(b5): $v = 0.353$ m/s, $We = 3.52$. (c1)–(c5): $v = 0.379$ m/s, $We = 4.05$. (d1)–(d5): $v = 0.403$ m/s, $We = 4.59$. (e1)–(e5): $v = 0.426$ m/s, $We = 5.12$. The solid substrate was PDMS membrane.

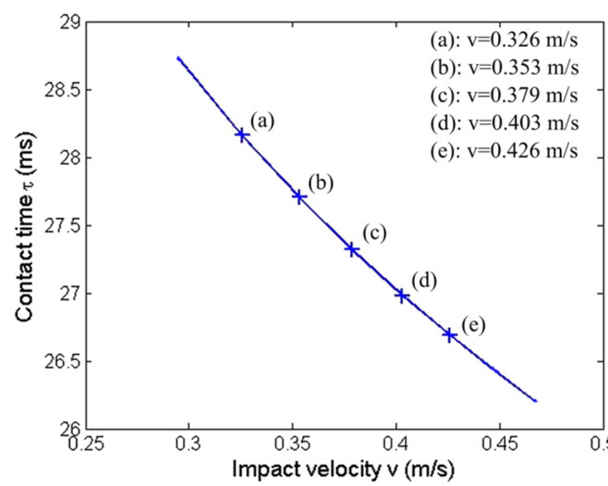

Fig. 7. Theoretical relationship between the contact time and the impact velocity. The marked data points in the diagram represent the theoretical solutions corresponding to the experimental results in Figs. 6a–6e, respectively.

5. Summary

In this paper, the head-on collision of the binary liquid droplets is studied experimentally and analyzed with a theoretical model. Responses after the collision can be distinguished into four cases: complete rebound, coalescence, partial rebound after conglutination, and coalescence accompanied by conglutination. Hertz contact theory is used to estimate the contact time. The analytical results are on the same order of magnitude as the experimental data, which indicates that the theoretical model is reasonable.

The authors believe that the droplet collision dynamics will remain an attractive scientific problem for a long time and more attention should be paid due to its various applications from aerospace to nanotechnology.

Acknowledgments

This work was jointly supported by the National Basic Research Program of China (973 Program, Grant No. 2007CB310500) and National Natural Science Foundation of China (NSFC, Grant No. 10772180).

References

[1] L. Rayleigh, The Theory of Sound, Dover Publication, New York, 1945.
[2] L. Rayleigh, Proc. R. Soc. London 29 (1879) 71–97.
[3] R. Guigon, J.J. Chaillout, T. Jager, G. Despesse, Smart Mater. Struct. 17 (2008) 015039.
[4] J. Berthier, Microdrops and Digital Microfluidics, William Andrew Publishing, New York, 2008.
[5] M. Rein, Fluid Dyn. Res. 12 (1993) 61–93.
[6] A.L. Yarin, Annu. Rev. Fluid Mech. 38 (2006) 159–192.
[7] S. Chandra, C.T. Avedisian, Proc. R. Soc. London A 432 (1991) 13–41.
[8] R. Rioboo, C. Tropea, M. Marengo, Atomization Sprays 11 (2001) 155–165.
[9] D. Richard, D. Quere, Europhys. Lett. 50 (2000) 769–775.
[10] Z. Wang, C. Lopez, A. Hirsa, N. Koratkar, Appl. Phys. Lett. 91 (2007) 023105.
[11] A.L. Biance, F. Chevy, C. Clanet, G. Lagubeau, D. Quere, J. Fluid Mech. 554 (2006) 47–66.
[12] D. Richard, C. Clanet, D. Quere, Nature 417 (2002) 811.
[13] K. Okumura, F. Chevy, D. Richard, D. Quere, C. Clanet, Europhys. Lett. 62 (2003) 237–243.
[14] J. Qian, C.K. Law, J. Fluid Mech. 331 (1997) 59–80.
[15] A.B. Wang, C.C. Chen, Phys. Fluids 12 (2000) 2155–2158.
[16] S.L. Manzello, Exp. Fluids 32 (2002) 580–589.
[17] R. Rioboo, C. Bauthier, J. Conti, M. Voue, J. De Coninck, Exp. Fluids 35 (2003) 648–652.
[18] K.L. Pan, C.K. Law, J. Fluid Mech. 587 (2007) 1–22.
[19] D. Bodas, C. Khan-Malek, Microelectron. Eng. 83 (2006) 1277–1279.
[20] J.T. Feng, Y.P. Zhao, Biomed. Microdevices 10 (2008) 65–72.
[21] J.T. Feng, Y.P. Zhao, J. Phys. D: Appl. Phys. 41 (2008) 052004.
[22] W. Dai, Y.P. Zhao, Int. J. Nonlinear Sci. Numer. Simul. 8 (2007) 519–526.
[23] G.B. Foote, J. Atmos. Sci. 32 (1975) 390–402.
[24] S.T. Thoroddsen, K. Takehara, Phys. Fluids 12 (2000) 1265–1267.
[25] Y. Renardy, S. Popinet, L. Duchemin, M. Renardy, S. Zaleski, C. Josserand, M.A. Drumright-Clarke, D. Richard, C. Clanet, D. Quere, J. Fluid Mech. 484 (2003) 69–83.
[26] N. Bremond, A.R. Thiam, J. Bibette, Phys. Rev. Lett. 100 (2008) 24501.
[27] S.T. Thoroddsen, T.G. Etoh, K. Takehara, J. Fluid Mech. 478 (2003) 125–134.
[28] S.T. Thoroddsen, J. Sakakibara, Phys. Fluids 10 (1998) 1359–1374.
[29] H.J. Hertz, Reine Angew. Math. 92 (1881) 156–171.
[30] L.D. Landau, E.M. Lifschitz, Theory of Elasticity, Pergamon Press, Oxford, 1986.